03.5

Map of water-oil flow regimes in a direct microchannel

© M.I. Pryazhnikov[1,2], A.V. Minakov[1,2], A.I. Pryazhikov[1], A.S. Yakimov[1]

[1] Siberian Federal University, Krasnoyarsk, Russia
[2] Kutateladze Institute of Thermophysics, Siberian Branch, Russian Academy of Sciences, Novosibirsk, Russia
E-mail: mpryazhnikov@sfu-kras.ru

Received September 21, 2021
Revised October 13, 2021
Accepted October 15, 2021

The flow regimes of water and crude oil in a Y-type microchannel were studied in a wide range of flow rates. Four different types of water-oil flow regimes have been identified: plug, droplet, parallel and chaotic. The ranges of existence of these flow regimes have been determined. Dependences of the length of water plugs and droplets in oil on various parameters have been established. Maps of the corresponding water-oil flow regimes have been constructed.

Keywords: Y-microchannel, liquid-liquid flow, immiscible liquids, flow regime map

DOI: 10.21883/TPL.2022.02.53572.19030

Flows of immiscible liquids are widespread in nature and technology. The study of flow regimes of immiscible liquids is especially important in problems concerning the displacement of oil upon reservoir flooding. It is known that various methods for enhanced oil recovery are based on the adjustment of flow regimes of oil and displacing liquids. The enhancement of oil recovery from a microporous medium depends on the pattern of flow in the pore space. The flow pattern in a microporous medium is, in turn, governed by several parameters: geometry (characteristic size and type of junctions between microchannels of the porous medium), the physical properties of oil, and the properties of liquid for enhanced oil recovery.

Although a considerable number of papers [1,2] focused on the flow of oil in microporous media have already been published, systematic data on the corresponding flow regimes are still insufficient. The number of factors influencing the flow regimes in oil recovery is so large that their further examination is required. In view of this, the aim of the present study is to examine systematically the regimes of water and oil flow in a direct microchannel imitating a pore. Microfluidic technology, which is applied often in current studies of flows in the case of displacement of oil from a porous medium [3,4], was used for this purpose.

The study was performed using a microfluidic chip with a Y-type microchannel (Fig. 1, *a*). The chip was fabricated from poly(methyl methacrylate) by milling and thermal sintering. Width w and height h of the microchannel were 500 and 200 μm, its length was 20 mm, and the length and the width of inlet regions were 5 mm and 250 μm (see the diagram in Fig. 1, *b*). Distilled water and light low-viscosity oil ($825 \pm 3\,\mathrm{kg \cdot s^{-1}}$, $8.5 \pm 0.2\,\mathrm{mPa \cdot s}$) were used in experiments. The interfacial tension measured with a tensiometer at the water–oil interface was $22.5 \pm 0.1\,\mathrm{mN \cdot m^{-1}}$ [5]. The equilibrium value of the interface angle was $124 \pm 2°$. Water and oil were pumped into the microfluidic chip with syringe pumps that allowed us to set the flow rate with a relative error of 0.5%. The microchannel was positioned horizontally on the object table of a microscope. The microchannel inlets were connected to syringes (Hamilton) via polypropylene tubes with an inner diameter of 1.2 mm. Volumetric flow rate Q was set. The flow pattern was monitored with a high-speed camera. Traditional parameters were used to characterize the flow regimes. The Reynolds number defines the ratio of inertia forces to viscous forces: $\mathrm{Re} = \frac{\rho U D}{\mu}$, where ρ is the density of liquid, U is the characteristic velocity, $D = 286\,\mu$m is the hydraulic diameter of the channel, and μ is the dynamic liquid viscosity. The Weber number characterizes the balance between inertia forces and surface tension forces: $\mathrm{We} = \frac{\rho U^2 D}{\sigma}$, where σ is the surface tension. The capillary number defines the relation between viscous forces and surface tension forces: $\mathrm{Ca} = \frac{\mu U}{\sigma}$. Another dimensionless number is the Ohnesorge number that is equal to the ratio between viscous forces and surface tension forces: $\mathrm{Oh} = \frac{\mu}{\sqrt{\rho \sigma D}}$. Experiments were performed within wide ranges of variation of flow rates and dimensionless numbers. These variation ranges are given in the table.

Four different water–oil flow regimes in the Y microchannel were identified as a result of experiments: plug, droplet, parallel, and chaotic flows. Typical images of these flow regimes are presented in Fig. 2. The plug regime was observed at low oil and water flow rates. Water plugs formed in this regime in all experiments. Oil is the carrier medium, since it has better properties in terms of wetting the channel walls. Water acts as a dispersed phase. The separation of the dispersed phase into plugs is governed by interfacial tension. A water plug occupies almost the entire cross section of the microchannel with a very thin oil film remaining between the plug and the microchannel wall. With the water (dispersed phase) flow rate kept constant, the plug length decreased as the oil flow rate increased. The

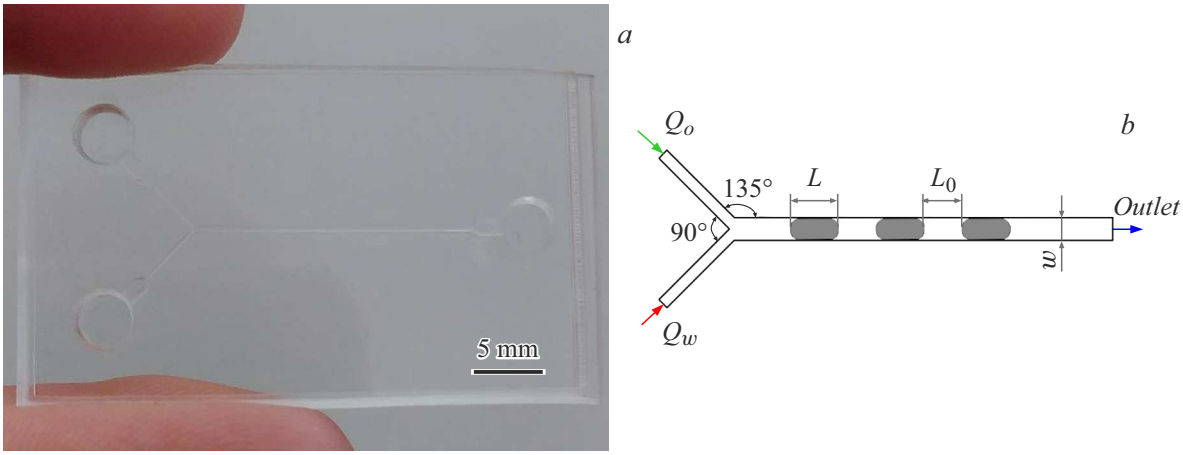

Figure 1. Photographic image of the microfluidic chip with a Y-type microchannel (a) and its diagram (b).

Ranges of variation of experimental parameters

Parameter	Water	Crude oil
Q, ml/h	$2.5 \cdot 10^{-2} < Q_w < 6.6 \cdot 10^2$	$10^{-1} < Q_o < 55$
Re	$2.2 \cdot 10^{-2} < \mathrm{Re}_w < 5.8 \cdot 10^2$	$7.7 \cdot 10^{-3} < \mathrm{Re}_o < 4.2$
We	$6.1 \cdot 10^{-8} < \mathrm{We}_w < 43$	$9.5 \cdot 10^{-8} < \mathrm{We}_o < 2.8 \cdot 10^{-2}$
Oh	$1.12 \cdot 10^{-2}$	$1.17 \cdot 10^{-1}$
Ca	$2.8 \cdot 10^{-6} < \mathrm{Ca}_w < 7.3 \cdot 10^{-2}$	$1.1 \cdot 10^{-4} < \mathrm{Ca}_o < 5.7 \cdot 10^{-2}$

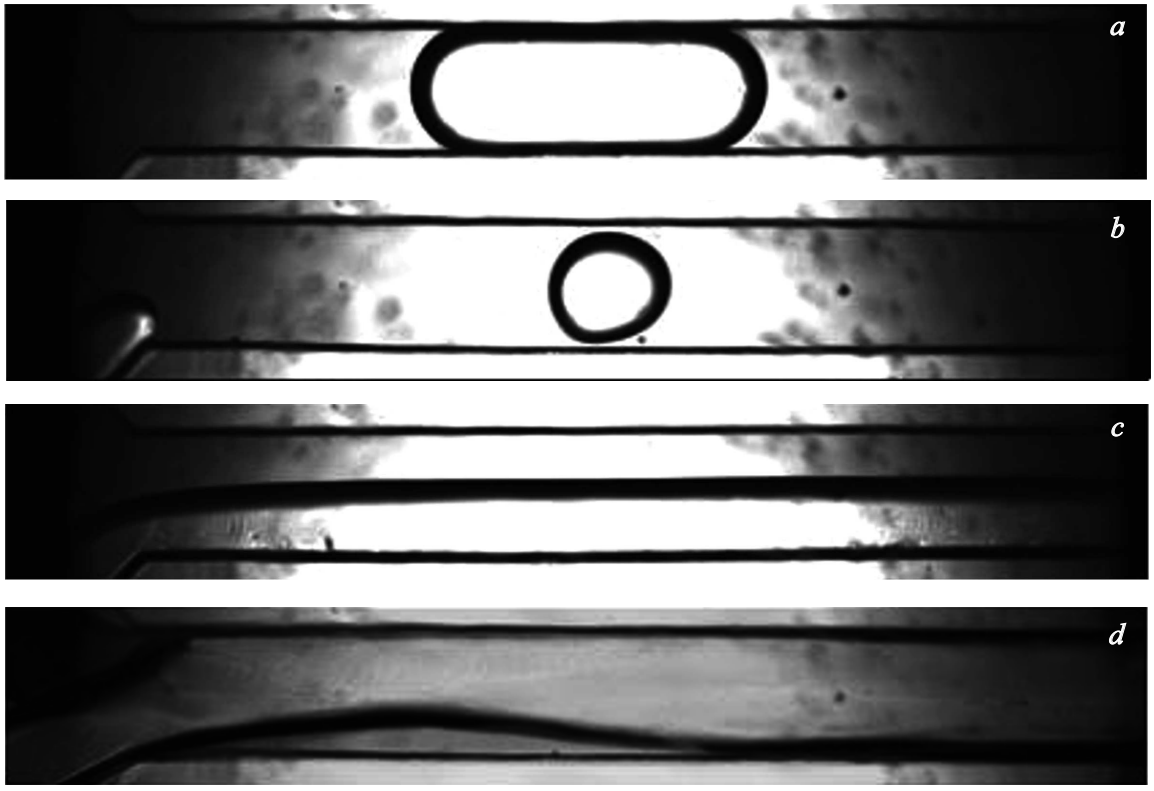

Figure 2. Observed flow regimes: a — plug, b — droplet, c — parallel, d — chaotic.

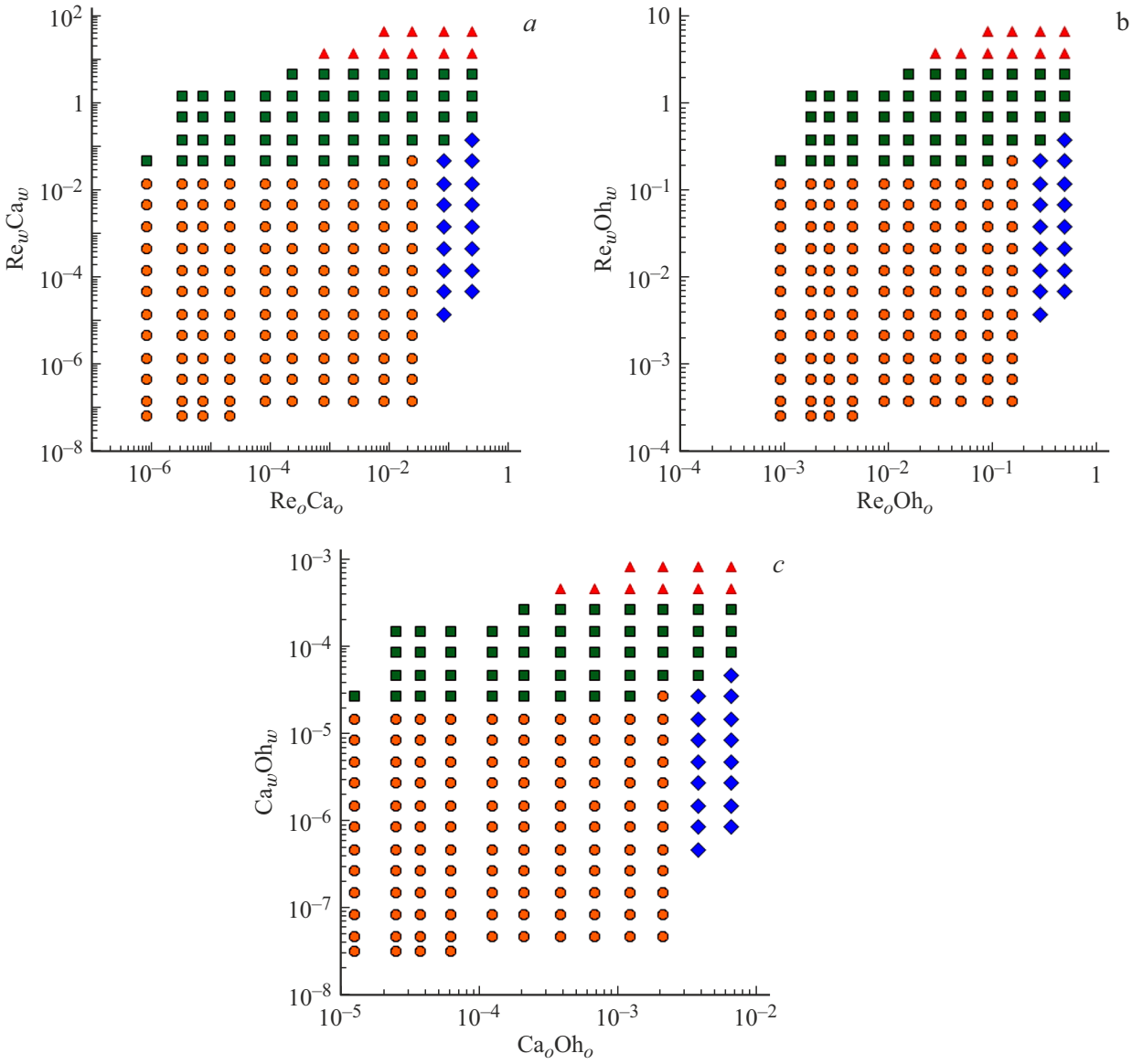

Figure 3. Map of water−oil flow regimes in coordinates of combined dimensionless numbers ReCa (*a*), ReOh (*b*), and CaOh (*c*). Squares, circles, diamonds, and triangles correspond to parallel, plug, droplet, and chaotic flow regimes, respectively.

same trend was observed at a constant oil flow rate and a decreasing water flow rate.

The following correlation characterizing plug length L was obtained by analyzing the experimental data:

$$\frac{L}{D} = \varepsilon + k\left(\frac{Q_d}{Q_c}\right)^{\alpha}\left(\frac{1}{\mathrm{Ca}_c}\right)^{\beta}, \qquad (1)$$

where $\varepsilon = 1.72$, $k = 1.45$, $\alpha = 0.525$, and $\beta = 0.138$ are the correlation parameters determined using the least-squares method; indices d and c denote the dispersed and carrier phases, respectively.

When the oil flow rate increased further, the flow regime changed to the droplet one. Water droplets in this regime were smaller than the microchannel in size (Fig. 2, *b*). This regime was established at high oil flow rates and low water flow rates. The formation of water droplets is attributable to the strong influence of inertia forces that emerge at high oil flow rates. Just as in the plug regime, the dimensionless length of droplets in the droplet flow regime is characterized well by correlation (1). The parameters of correlation (1) for the droplet flow regime are as follows: $\varepsilon = 1.17$, $k = 0.0926$, $\alpha = 0.412$, and $\beta = 0.936$.

At higher oil and water flow rates, the inertia force dominates over the force of interfacial tension, and liquids flow parallel to each other without the formation of plugs or droplets. This is the so-called parallel flow regime presented in Fig. 2, *c*. Our experiments demonstrated that the position of the interface between oil and water inside the microchannel changes as the oil and water flow rates vary.

When the water flow rate increased further, parallel flow gave way to chaotic flow (Fig. 2, *d*). This regime is established at very high oil and water flow rates. Multidimensional flow forms at high velocities of oil and water under the influence of centrifugal forces. Oil and water flows in this regime turn over in the mixing channel and then flow in the parallel regime along opposite walls. Similar behavior was observed in the case of single-phase liquid flow in a *T*-type microchannel. The results of systematic studies of single-phase flow in a *T*-type microchannel at high Reynolds numbers were presented in [6]. A pair of symmetric horseshoe vortices form as a result of development of secondary Dean flow and decay in the microchannel. Notably, each of these vortices is located within the same liquid (oil or water). Starting from a Reynolds number equal approximately to 145, the pair of horseshoe vortices turns at an angle of 30° to the central longitudinal plane of the microchannel. As a result, one vortex decays, while the other is intensified. A similar pattern is observed in the present case. Oil and water flows also turn over in the mixing channel.

Water–oil flow in a *Y*-type microchannel was examined experimentally in the present study. A map of flow regimes was obtained. The following four different flow regimes were observed: parallel, droplet, plug, and chaotic flows. The map of water–oil flow regimes was plotted in the coordinates of combined Reynolds, Ohnesorge, and capillary numbers (Fig. 3). No consensus exists presently regarding the choice of parameters to be used as coordinates for maps of flow regimes for two-phase flows in microchannels. Velocities or flow rates of phases were used in a number studies (mostly the ones published earlier) to characterize the flow regime [7,8]. The Reynolds number is also used often for classification of flow regimes [8]. The map of flow regimes in [9] was plotted against the Weber number. Combinations of dimensionless numbers raised to certain powers are often used to characterize flow regimes. In the present study, flow regimes were characterized with the following combinations of dimensionless numbers: Reynolds and capillary numbers (Fig. 3, *a*), Reynolds and Ohnesorge numbers (Fig. 3, *b*), and capillary and Ohnesorge numbers (Fig. 3, *c*). These parameters are the most convenient for problems concerning the enhancement of oil recovery.

Thus, the water–oil flow regimes in a direct microchannel imitating a pore were studied in a microfluidic experiment. The ranges of existence of different regimes were determined. Dependences of the length of water plugs and droplets in oil on the ratio of water and oil flow rates and on the capillary number calculated for the carrier phase were determined. Maps of the corresponding water–oil flow regimes were plotted. These data should help in the development of techniques for enhanced oil recovery.

Acknowledgments

The authors would like to thank the Krasnoyarsk Regional Common Use Center (Krasnoyarsk Scientific Centre of the Siberian Branch of the Russian Academy of Sciences).

Funding

This study was performed under state assignment for the Siberian Federal University (No. FSRZ-2020-0012).

Conflict of interest

The authors declare that they have no conflict of interest.

References

[1] A. Perazzo, G. Tomaiuolo, V. Preziosi, S. Guido, Adv. Coll. Interface Sci., **256**, 305 (2018). DOI: 10.1016/j.cis.2018.03.002
[2] J. Foroozesh, S. Kumar, J. Mol. Liq., **316**, 113876 (2020). DOI: 10.1016/j.molliq.2020.113876
[3] M. Saadat, J. Yang, M. Dudek, G. Øye, P.A. Tsai, J. Pet. Sci. Eng., **203**, 108647 (2021). DOI: 10.1016/j.petrol.2021.108647
[4] X. Zhao, Y. Feng, G. Liao, W. Liu, J Coll. Interface Sci., **578**, 629 (2020). DOI: 10.1016/j.jcis.2020.06.019
[5] A.V. Minakov, M.I. Pryazhnikov, Y.N. Suleymana, V.D. Meshkova, Tech. Phys. Lett., **46** (12), 1238 (2020). DOI: 10.1134/S1063785020120238.
[6] A.S. Lobasov, A.V. Minakov, Chem. Eng. Process. — Process Intensif., **124**, 11 (2018). DOI: 10.1016/j.cep.2017.11.004
[7] I. Mudawar, J. Electron. Packag. Trans. ASME, **133** (4), 041002 (2011). DOI: 10.1115/1.4005300
[8] H. Foroughi, M. Kawaji, Int. J. Multiphase Flow., **37** (9), 1147 (2011). DOI: 10.1016/j.ijmultiphaseflow.2011.06.004
[9] Y. Zhao, G. Chen, Q. Yuan, AIChE J., **52** (12), 4052 (2006). DOI: 10.1002/aic.11029